European Biophysics Journal
https://doi.org/10.1007/s00249-018-1293-3

ORIGINAL ARTICLE

Ferritin from the haemolymph of adult ants: an extraction method for characterization and a ferromagnetic study

Eliane Wajnberg[1] · Odivaldo C. Alves[2] · Jonas Perales[4] · Surza Lucia G. da Rocha[4] · André Teixeira Ferreira[4] · Luiz Cláudio Cameron[3] · Darci M. S. Esquivel[1] · Maria de Lourdes Barriviera[1]

Received: 1 November 2017 / Revised: 5 February 2018 / Accepted: 13 March 2018

Abstract

Ferritin has been studied in many animals, plants and bacteria. The main functions of ferritin in mammals are iron concentration and stabilization, protection against oxidants and iron storage for later developmental or iron-dependent activities. Although insect ferritin plays a key role in iron transport, only a few studies to date have examined its properties and function. Ferritin isolation from the haemolymph of adult *Camponotus sericeiventris* ants involved heating at 75 °C, followed by protein fractionation with 3.2 M KBr gradients and ferritin sedimentation with KBr. Protein identification was performed using high-resolution proteomics techniques. SDS-PAGE revealed three subunits with molecular weights (MW) of 26, 28 and 31 kDa. Native PAGE indicated a MW higher than 669 kDa. Proteomic analysis strongly suggested the 26 and 31 kDa bands as F2LCH and F1HCH subunits of ferritin, respectively. Ferromagnetic resonance (FMR) at 100 K showed, at low field, a characteristic broad component of the ferritin iron core, suggesting that its distribution was shifted to values greater than 3000, a higher content than in mammals. The protein yield and MW were comparable to those reported in other studies of insects. To the best of our knowledge, this is the first report on ferritin extracted from adult ants to date. These results are discussed on the basis of the protein structure–function relation of secreted insect and mammal ferritins. This purification method will allow the use of magnetic techniques, which are relevant for understanding the role of ferritin in the biomineralization of magnetic nanoparticles in insects.

Keywords Ferritin · Eusocial insect · Ants · Ferromagnetic resonance (FMR) · Iron transport

Introduction

Ferritin is a protein found throughout the animal and plant kingdoms and in microorganisms. Its function in iron metabolism varies within the animal kingdom (Arosio et al. 2009), but is primarily iron storage and stabilization and antioxidant protection (Arosio et al. 2015). Ferritin is mostly studied in mammals, in which it is found mainly in the cytoplasm of cells, though a secreted form of ferritin is also found in the serum and is a clinically important measure of iron stores in anaemia, inflammation, infection, liver function, cancer and oxidative stress (Cohen et al. 2010; Pham and Winzerling 2010; Wang et al. 2010 and references therein). In contrast, few studies have examined insect ferritin, of which most have focused on moths and butterflies, which are of agricultural importance, flies and mosquitoes for their role as disease vectors, and *Drosophila* as a biological model. Interestingly, insect ferritin is mainly present extracellularly in μg/mL quantities (higher than the concentration of

Electronic supplementary material The online version of this article (https://doi.org/10.1007/s00249-018-1293-3) contains supplementary material, which is available to authorized users.

✉ Eliane Wajnberg
elianew@cbpf.br

[1] Coordenação de Materiais, Física Aplicada e Nanociências, Centro Brasileiro de Pesquisas Físicas, R. Dr. Xavier Sigaud 150, Rio de Janeiro, RJ 22290-180, Brazil

[2] Departamento de Físico-Química, Universidade Federal Fluminense, Niteroi, RJ, Brazil

[3] Laboratório de Bioquímica de Proteínas, Universidade Federal do Estado do Rio de Janeiro, Rio de Janeiro, RJ, Brazil

[4] Laboratório de Toxinologia, Instituto Oswaldo Cruz, Fundação Oswaldo Cruz, Rio de Janeiro, RJ, Brazil

Published online: 28 March 2018

vertebrate plasma ferritin) (Ong et al. 2006). It was shown to exist in association within the vacuolar system of the fat body where it is secreted into haemolymph (Hajdusek et al. 2009; Nichol et al. 2002). Studies of iron metabolism have demonstrated its relevance (Tang and Zhou 2013) in iron transport to peripheral tissues, which is uncommon among vertebrate ferritins, and with significant roles in the immune response as in vertebrates (Ong et al. 2006; Pham and Winzerling 2010 and references therein).

The three-dimensional structure of eukaryotic ferritins is well conserved throughout the animal and plant kingdoms and consists of a spherical molecule with octahedral symmetry composed of 24 subunits, with a cavity that accommodates up to 4500 iron atoms (Arosio et al. 2015; Tang and Zhou 2013; Hamburger et al. 2005). In vertebrates, ferritin is composed of two different but very similar peptide subunits, the H-chain and L-chain with a flexible H:L ratio, depending on the tissue from which it has been isolated (Wagstaff et al. 1978). The H-chain is identified by the presence of seven conserved amino acid residues that are responsible for the ferroxidase activity of these subunits. The L-chain is responsible for facilitating iron core formation inside the protein shell. Insect ferritins are composed of two homologues of the vertebrate H and L subunits (F1HCH and F2LCH) (Dunkov and Georgieva 2006), although there are reports of up to five subunit types in some species (Seo et al. 2004; Kim et al. 2001b). The subunits are often glycosylated, with higher molecular weights than those of vertebrates, resulting in a total MW of 400–600 kDa (Capurro et al. 1996; Huebers et al. 1988; Nichol and Locke 1989; Winzerling et al. 1995).

Physicochemical studies of insect ferritin have been predominantly based on the extracted protein from haemolymph in the larval phase from *Calpodesethlius*, *Manduca sexta*, *Drosophila melanogaster*, *Musca domestica* (Capurro et al. 1996; Huebers et al. 1988; Nichol and Locke 1989; Winzerling et al. 1995; Charlesworth et al. 1997) and confirmed via immunological analysis and amino acid sequencing (Kim et al. 2001a, 2004). To the best of our knowledge, there are no studies on ferritin from adult insect haemolymph. More recently, ferritin studies have involved the use of proteins prepared by recombinant and cloning methods, but it is relevant to note that protein core loading and/or shell loading differ from the native ferritin (Kim et al. 2001a; Bradley et al. 2016).

The nature of the ferritin iron mineral core has been the focus of numerous studies using a wide variety of physical and chemical techniques. X-ray diffraction revealed two- and six-line diffraction patterns, indicating ferrihydrite mineral composition (Chasteen and Harrison 1999). Later on, iron was gradually removed from the core with thioglycolic acid and the core examined using spectroscopic and magnetic techniques. Ferrihydrite, magnetite, and haematite were shown to be present in relative fractions that depended on the iron content (Gálvez et al. 2008) which agrees with the three-phase model proposed for the magnetization curves of ferritin (Jung et al. 2011). Although ferritin has been isolated from a wide variety of sources, the morphologies and the core size distribution in vertebrates were generally not reported, except for Pierre et al. (1991), likely because electron microscopy (EM) and Mossbauer facilities were not as available as they are now (Alenkina et al. 2014). Uncommonly, in insects, the size distribution of the core in *Musca* was suggested based on the iron content of ferritin fractions obtained from the glycerol gradient (Capurro et al. 1996) and more recently, iron loading and three-dimensional maps of the *Drosophila* ferritin shell and core were obtained from magnetic analysis and EM, respectively (Gutiérrez et al. 2013). Other review articles describe relevant studies in insect ferritin (Tang and Zhou 2013; Mandilaras et al. 2013).

Magnetic particles have been reported in the body parts of social insects mainly using magnetic techniques, such as ferromagnetic resonance (FMR) and superconducting quantum interference device (SQUID) magnetometry (Wajnberg et al. 2010). In particular, the presence of magnetic particles in the abdomen of honeybees (*Apis mellifera*) (Gould et al. 1978; Kuterbach and Walcott 1986; Hsu and Li 1994), has led to controversial conclusions on their composition, magnetite or ferritin. Hsu and collaborators established a size-density purification procedure to recover adequate amounts of iron granules (IGs) from trophocytes for characterization and to demonstrate the presence of magnetite in these IGs and a model for magnetite biomineralization (Hsu et al. 2007; Hsu and Chan 2011). A precise magnetic characterization of ferritin for comparison with other magnetic materials in the body parts of social insects remains an interesting open question.

In this study, adult ants were used because magnetoreception is most relevant during this phase and the presence of magnetic particles as possible sensors has been demonstrated previously (Wajnberg et al. 2010). Ferritin was isolated from the haemolymph of adult arboreal ants (*Camponotus sericeiventris*) using biochemistry methods. High-resolution proteomics techniques were used to identify the protein subunits. Finally, ferritin was magnetically characterized using FMR.

Materials and methods

Social insects

Arboreal carpenter ants (*Camponotus sericeiventris*) were collected from the soil, close to their nest or directly from the nest cavity of trees at the Centro Brasileiro de Pesquisas Físicas (CBPF), Rio de Janeiro, Brazil.

Haemolymph collection

About one hundred ants were placed in the refrigerator to decrease their activity. Later, the ants were washed in distilled water, 70% alcohol and cold phosphate buffered saline. The head and thorax were separated, pressed and the haemolymph was collected using a micro-syringe and diluted with equal volumes of cold anticoagulant buffer: Tris–HCl 80 mM (pH 6.8), 0.15 M NaCl; 0.1 mM EDTA; 1 mM phenylmethylsulfonyl-fluoride (PMSF) and 0.2% phenylthiourea (PTU). [PTU (1 g) was dissolved in acetone (1 mL) and added to 500 mL of buffer solution].

The ants were collected, and their body parts were separated. The intact thoraxes (4 units) and heads (5 units) were washed with ethanol and dried for 30 min at 50 °C just before FMR analysis.

Protein determination

Protein concentrations were determined using Qubit, a commercially available fluorometric quantisation protocol (Qubit® Fluorometer—Invitrogen).

Polyacrylamide gel electrophoresis

The efficiency of the purification steps and the MW of the ferritin subunits were assessed with SDS-PAGE, performed using 12% gels with 0.1% SDS according to the procedure of Laemmli (1970). The gels were stained with Coomassie brilliant blue G-250 solution and silver nitrate. The purified protein was also analysed using native-PAGE carried out on a 4–20% gradient gel (Amershan ECL—GE Healthcare) using Tris–glycine buffer (pH 8.3).

The molecular mass of the ferritin subunits was assessed from the reducing SDS-PAGE gel described above. The standard molecular mass marker proteins used were phosphorylase b (97.4 kDa), serum albumin (66.2 kDa), ovalbumin (45 kDa), carbonic anhydrase (31 kDa), trypsin inhibitor 21.4 kDa) and lysozyme (14.4 kDa) and were obtained from Bio-Rad. The molecular mass was estimated from the interpolation of a log MW × relative mobility (Rf) curve, using Ferguson plot (Werner 1995).

Iron staining

The presence of Fe in the native holoferritin was confirmed by immersing the gels for at least 15 min in a specific staining solution consisting of 0.75 mM 3-(2-pyridyl)-5,6-bis (2-(5-furyl sulfonic acid)-1,2,4-triazine, disodium salt (Ferene S) and 15 mM thioglycolic acid in 2% (v/v) acetic acid. The solvent was prepared immediately before it was used according to Chung (1985).

Ferritin isolation

The purification procedure was adapted from previously published methods used to obtain ferritin from larval insects (Capurro et al. 1996; Nichol and Locke 1989; Winzerling et al. 1995), except for the iron addition step that was not used here. The main modification to the protocol was the order of the steps, where the heat-treatment was performed as the first step and two density gradient ultracentrifugation were performed immediately after. The haemocytes and debris of the diluted haemolymph were removed via centrifugation at 11,000*g* (10 min, 10 °C), heated at 75 °C for 30 min in a water bath, and then centrifuged at 11,000*g* (10 min, 10 °C).

Attempts to eliminate higher molecular weight proteins were performed by adding either 1% sodium dodecyl sulphate (Nichol and Locke 1989) or protein proteinase K (Atkinson et al. 1989) to the supernatant after heat treatment.

The supernatant was submitted to 3.2 M KBr (0.445 g/mL solution) density gradient ultracentrifugation at 105,000*g* for 16 h at 10 °C in an SW-55 Ti rotor (Beckman model Cooter Optima L100 K). The clear supernatant was removed and the pellet at the bottom of the tube was resuspended in 0.05 M phosphate buffer (pH 7.0). The density was adjusted to 1.37 g/mL using solid KBr (20 °C). This solution was pooled into a rotor tube and underlayered with KBr with a density of 1.375 g/mL for ultracentrifugation (180,000*g*, 18 h, 20 °C). The resulting pellet was solubilised in 100 µL of 0.05 M phosphate buffer (pH 7.0).

The first attempts to isolate ferritin from the haemolymph of adult ants were performed using chromatographic methods (Seo et al. 2004; Kim et al. 2004) rather than ultracentrifugation. Briefly, the supernatant was submitted to gel filtration (FPLC system, Pharmacia) in a Superose 6 HR 10/30 column. The proteins were eluted with 25 mM sodium tetraborate (pH 9.0) at a flow rate of 0.15 mL/min in a 1 mL fraction. The proteins were eluted with 50 mM Tris–HCl buffer (pH 8.0) followed by a linear gradient 0–0.5 M at a flow rate of 0.5 mL/min (1.0 mL-fraction) in an anion exchange column (FPLC system, Pharmacia) placed in a Mono-Q column.

In-gel tryptic digestion

Protein bands in the 21–45 kDa and 66–97 kDa range separated on the SDS-PAGE after the 1st gradient ultracentrifugation were excised from the gel using sterile stainless steel scalpels, transferred to 0.5 mL tubes and cut into smaller pieces. Digestion was performed using trypsin (Promega

V511A) according to methods described by Shevchenko et al. (1996).

Silver nitrate-stained samples were destained by adding 200 µL of a 1:1 (v/v) 30 mM potassium ferricyanide/100 mM sodium thiosulphate.

The Coomassie-stained samples were destained with 0.025 M ammonium bicarbonate for 15 min and then discarded. This washing procedure was repeated until the destaining was complete, which was determined through visual inspection.

The washing solution was then removed, and the gel was dehydrated by adding 200 µL of acetonitrile for 5 min. The solvent was removed, and the samples were completely dried in a vacuum centrifuge. Each sample was rehydrated with 15 µL of ice-cold trypsin solution (20 ng/µL in 40 mM ammonium bicarbonate, pH 8.0) and left on ice for 45 min. After gel reswelling, 20 µL of 40 mM ammonium bicarbonate was added to the samples followed by incubation for 16 h at 37 °C. Following digestion, the peptides were transferred to new 0.5 mL tubes and the gel was re-extracted by adding 30 µL of 1:1 (v/v) 5% formic acid/50% acetonitrile and ultrasonification for 10 min. The re-extracted solution was added to the first extracted solution, concentrated to 10 µL and stored at − 20 °C for later use.

Sample desalting

C18 Zip-Tip 10 µL Millipore micropipette tips were used to desalt the peptides. The tips were first activated with 50% acetonitrile in water and then equilibrated with 0.1% TFA in water. The samples were aspirated and dispensed for eight cycles. The tips were washed with 0.1% TFA in water ten times. The peptides retained on the tips were eluted using 1.5 µL of 50%/0.1% (v/v) TFA in water.

Protein identification using high-resolution Orbi/Trapmass spectrometry

Reversed-phase nanochromatography coupled with nanoelectrospray high-resolution mass spectrometry was performed for tryptic digest identification. For each sample, 4 µL of desalted tryptic peptide digest were initially applied to a 2 cm long (100 µm internal diameter) trap column packed with 5 µm of 200 A Magic C18 AQ matrix (Michrom Bioresources, USA) followed by separation on a 10 cm long (75 µm internal diameter) separation column that was packed with the same matrix directly on a self-pack 15 µm PicoFrit empty column (New Objective, USA). Chromatography was carried out on an EASY-nLC II instrument (Thermo Scientific, USA). The samples were loaded onto the trap column at 2000 nl/min, while chromatographic separation occurred at 200 nl/min. Mobile phase A consisted of 0.1% (v/v) formic acid in water. Mobile phase B consisted of 0.1% (v/v) formic acid in acetonitrile. The gradient conditions were as follows: 2–40% B for 32 min and up to 80% B for 4 min. This concentration was maintained for 2 min more before the column was re-equilibrated. The eluted peptides were directly introduced to an LTQ XL/Orbi/Trap MS (Thermo, USA) for analysis. The voltage source was set to 1.9 kV, the capillary temperature to 200 °C and the tube lens voltage to 100 V. The full ion trap value and the MSn AGC target value was 30,000 and 10,000, respectively. The FTMS full AGC target value was set to 500,000. The MS1 spectra were acquired on the Orbitrap analyser (300–1700 *m*/*z*) at a 60,000 resolution (for *m*/*z* 445.1200). For each spectrum, the 10 most intense ions were submitted to CID fragmentation (minimum signal required of 10,000; isolation width of 2.5; normalized collision energy of 35.0; activation Q of 0.25 and activation time of 30 s) followed by MS2 acquisition on the linear trap analyser. The dynamic exclusion option was enabled. The parameter settings were as follows: repeat count = 1; repeat duration = 30 s; exclusion list size = 500; exclusion duration = 45 s and exclusion mass width = 10 ppm.

The peptide mass profiles were analysed using Peaks Studio (8.5 version). Searches were performed using the Formicidae database extracted from the UniProt Consortium (2017) (215.356 entries). Peaks search parameters for monoisotopic peptide masses allowed two missed enzymatic cleavages and accepted the carbamidomethylation of the cysteine residues with fixed modification and the oxidation of methionine as variable modification; the peptide tolerance 10 ppm (precursor) and fragment tolerance 0.60 Da. The protein identification results were confirmed with further statistical validation, using Scaffold software 4.8.3 version (Searle 2010).

Identification of ferritin F1HCH and F2LCH subunits

Multialin software (Corpet 1988) was used to perform the amino acid sequence alignment to identify the cysteine residues at different positions in the F1HCH and F2LCH subunits and conserved residues that form the ferroxidase activity center in the F1HCH.

Ferromagnetic resonance

The ferromagnetic spectra were obtained using a conventional Electron Paramagnetic Resonance X-band spectrometer (Bruker ESP300E) at RT and at 100 K with a helium flux system (Oxford instruments, ESR900). Approximately 20 µL of the native haemolymph and the resuspended purified solutions were used for the FMR measurements using at least 50 mW of microwave power. The spectra of the heads with the antennae and thoraxes of 5 ants were obtained using 100 mW of microwave power just after preparation. All spectra were acquired with a 10 G amplitude modulation.

The peak-to-peak linewidth, ΔH, and the *g* factor values expressed as $h\nu/\beta H$, where *h* is Plank's constant, ν the microwave frequency and *H* the field value at the half-height of the line, were obtained from the spectra using WinEPR software (Bruker).

Results

Ferritin isolation

Haemolymph obtained from the thoraxes and heads of 100 adult arboreal ants (*C. sericeiventris*) (1–3 µL haemolymph/ant) yielded a maximum of 0.5 mL of dilute native haemolymph, 1:1 (v/v haemolymph/buffer), with approximately 3 mg/mL of total protein. The haemolymph proteins were resolved into a minimum of 20 polypeptide bands using SDS-PAGE as shown in Fig. 1a.

Ferritin was not observed in the native-PAGE gel (not shown) after the addition of 1% SDS, to the heat-treated haemolymph of adult *C. sericeiventris* ants. SDS effectively removed most proteins with lower molecular weights and ferritin, however, it was unable to denature other proteins with high molecular weights, such as arylphorin, the major one. Similarly, the addition of proteinase K failed to eliminate proteins with high molecular weights (data not shown). We eliminated the step based on the resistance of ferritin to SDS (Nichol and Locke 1989) and digestion by proteinase K (Atkinson et al. 1989), because they did not confer any further improvement relative to the heating step, as observed by the electrophoresis fractions (figure not shown).

The electrophoretic pattern of the heat-treated adult insect haemolymph at 75 °C resulted in the decreased precipitation of non-resistant proteins (shown in Fig. 1b). Only a few bands were eliminated, most were only reduced relative to those found in the native haemolymph (Fig. 1a). The arylphorin subunit was significantly reduced. Its band position is indicated in Fig. 1, for which proteomic analysis revealed transferrin and arylphorin subunit peptides.

Previous studies used the FPLC method (Kim et al. 2001b, 2004); however, this method demands a high sample volume and a high protein concentration. Even though we were unable to obtain sufficiently large volumes and concentrations, we attempted column chromatography purification (gel filtration and anion exchange). The protein recovery from both columns was very low and was spread over a large range of tubes that were contaminated with other proteins. The low concentration of recovered ferritin was not adequate for further column purification.

To increase the purification efficiency, we applied the KBr density gradient ultracentrifugation method. The first KBr density ultracentrifugation procedure resulted in a visible brown precipitate fraction at the bottom of the tube. After

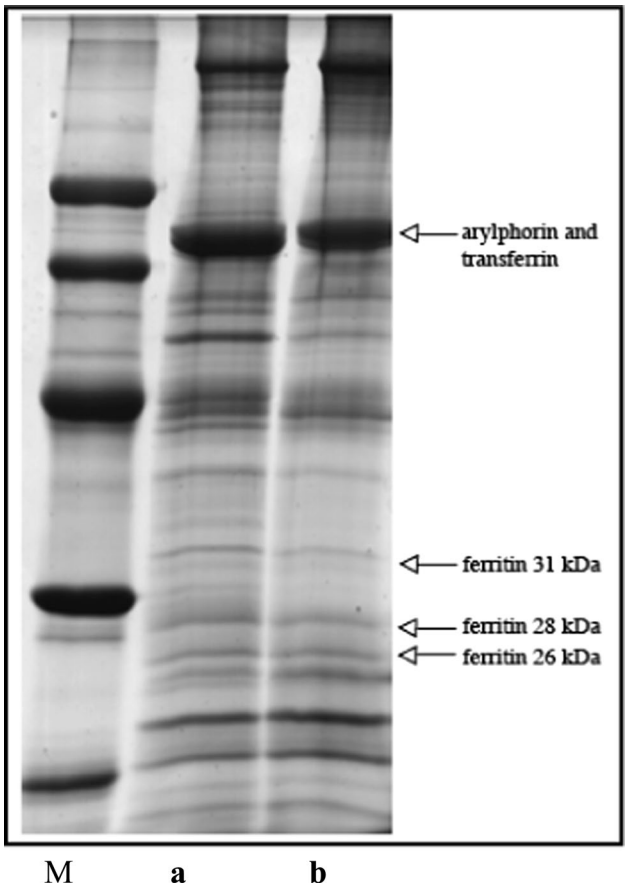

Fig. 1 SDS-PAGE electrophoretic patterns of proteins found in adult haemolymph extracted from the *C. sericeiventris* ant: a—total adult haemolymph; b—heat-treated (first purification step) haemolymph; M—protein size markers: phosphorylase b (97.4 kDa), serum albumin (66.2 kDa), ovalbumin (45 kDa), carbonic anhydrase (31 kDa), trypsin inhibitor (21.4 kDa) lysozyme (14.4 kDa). Arrows indicate the 26, 28 and 31 kDa bands further identified as ferritin subunits via proteomic analysis

the first and second KBr density ultracentrifugation procedures, the electrophoretic pattern (shown in Fig. 2) indicated that the components were eliminated gradually from the obtained precipitates. The MWs of the three remaining bands (Fig. 2, lane c) 26, 28 and 31 kDa were estimated from the interpolation of the Ferguson plot (inset in Fig. 2). These values are within the range of insect ferritin subunits.

The precipitate from the 2nd ultracentrifugation was analysed using non-denaturing gel electrophoreses. The top gel in Fig. 3 shows the destained gel re-stained with silver nitrate that confirmed the protein purification, subunits of which are indicated by the arrows in Fig. 2, lane c. The lower gel in Fig. 3 was stained with Ferene-S, a specific dye for iron, and exhibited only two blue bands: the horse ferritin standard, lane a and the only band in the purified sample (arrows in top and lower gel, lane b) with a MW higher than 669 kDa (thyroglobulin).

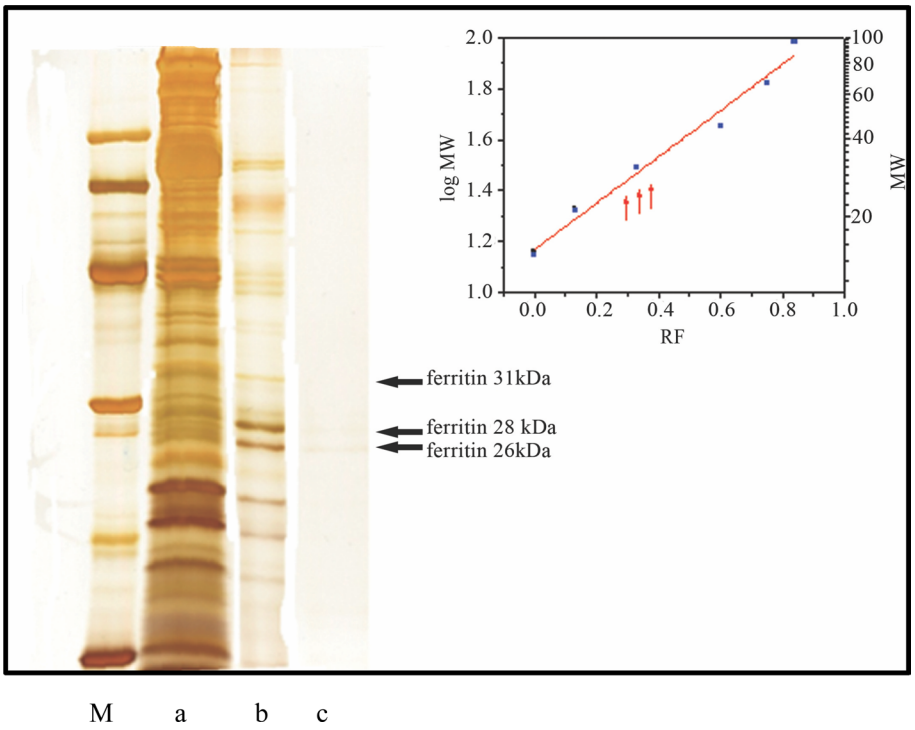

Fig. 2 SDS-PAGE electrophoretic patterns of the proteins found in the adult haemolymph after the purification steps of ferritin from the *C. sericeiventris* ant: a—adult total haemolymph; b—1st gradient density ultracentrifugation; c—2nd gradient density ultracentrifugation.; M—protein size marker (the marker proteins are the same as those shown in Fig. 1). Arrows indicate the 26, 28 and 31 kDa bands further identified as ferritin subunits via proteomic analysis. Inset: Determination of the polypeptide molecular weights of the 3 bands (indicated by the 3 arrows). The calibration curve was obtained with molecular weight markers for SDS-PAGE electrophoresis run on the same gel

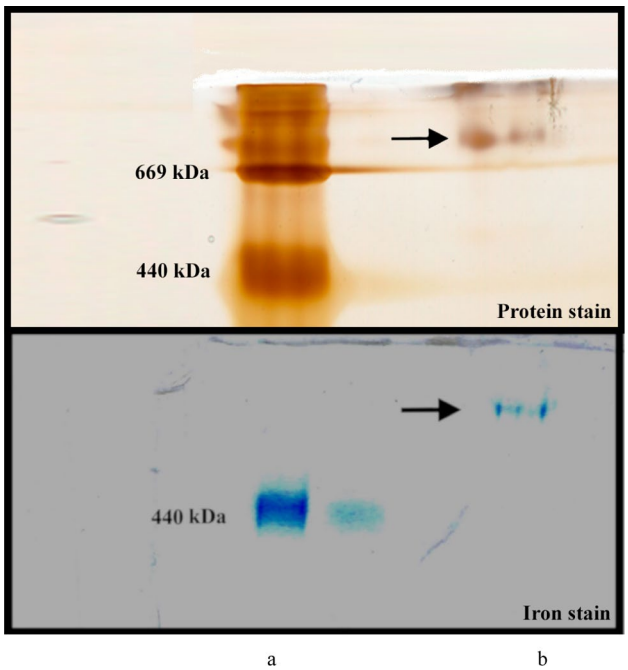

Fig. 3 4–20% gradient native-PAGE electrophoretic pattern of *C. sericeiventris* ant haemolymph after the 2nd ultracentrifugation: TOP GEL—stained with silver nitrate and LOWER GEL—stained with specific dye Ferene S. a—horse spleen ferritin (440 kDa) and thyroglobulin (669 kDa) were used as standard markers; b—high MW intact protein. Arrows indicate the ferritin band as confirmed by proteomic analysis

Table 1 shows the high-resolution proteomic analysis of the peptides obtained by Orbi/Trap MS from 26, 28 and 31 kDa bands excised from the SDS-PAGE gel that remained after the 1st gradient ultracentrifugation step (Fig. 2, lane b). Peak identification parameters of these peptides are summarised in Table 1 and given in more detail in Tables S1–S3 (Online Resource ESM1–3.pdf). Ferritin was the protein with the best Peaks score (higher than 95%), with a higher number of identified peptides than other suggested proteins. Despite the low peptide coverage percentage of the subunit sequence (15–35%), in all entries ferritin presents, at least, one unique peptide (Table 1 and Tables S1–S3 in Online Resource ESM1–3.pdf) that support the ferritin identification. Ferritin was assigned to be the main and exclusive protein for the analysed peptides. This analysis was statistically validated by scaffold that resulted in a 100% probability identification of ferritin and 0.3% of false discovery rate (FDR) for the three bands, based on a minimum of two peptides. For more details see the complete tables from the Peaks database (Tables S1–S3 in Online Resource ESM1–3).

Multialin software (Corpet 1988) was used to align the predicted amino acid sequence of the ferritin subunits from *Formicidae* species, for which UniProt Accession number sequences are presented in Table 1 and from *Drosophila melanogaster*. The peptides of the 26, 28 and 31 kDa obtained by Orbi/Trap MS that Peaks Studio that matched these sequences are underlined in Fig. 4.

Table 1 Identification of ferritin subunit peptides from the haemolymph of *Camponotus sericeiventris* ants by proteomic analysis

Access ion	Score (%)[a]	(− 10lgP)[b]	Coverage (%)[c]	Peptides counts	Unique peptides counts	Avg. mass	Description
26 kDa							
E2AZU1_CAMFO	99	166.99	21	8	8	24,959	Ferritin OS = *Camponotus floridanus* GN = EAG_15046 PE = 3 SV = 1
28 kDa							
E2AZU1_CAMFO	98.9	140.1	19	5	5	24,959	Ferritin OS = *Camponotus floridanus* GN = EAG_15046 PE = 3 SV = 1
A0A0J7KV83_LASNI	98.9	135.92	23	8	2	24,601	Ferritin OS = *Lasius niger* GN = RF55_5701 PE = 3 SV = 1
E2AZU0_CAMFO	96.8	118.49	26	6	5	18,973	Ferritin subunit OS = *Camponotus floridanus* GN = EAG_15045 PE = 4 SV = 1
31 kDa							
A0A195FTV1_9HYME	98.9	158.52	35	8	1	20,858	Ferritin OS = *Trachymyrmex septentrionalis* GN = ALC56_01623 PE = 3 SV = 1
A0A195C2H5_9HYME	98.9	158.52	29	8	1	24,975	Ferritin OS = *Cyphomyrmex costatus* GN = ALC62_14385 PE = 3 SV = 1
A0A158NNJ1_ATTCE	98.9	158.52	29	8	1	25,025	Ferritin OS = *Atta cephalotes* PE = 3 SV = 1
F4WEY7_ACREC	98.9	158.52	28	8	1	25,834	Ferritin OS = *Acromyrmex echinatior* GN = G5I_04191 PE = 3 SV = 1
A0A151X800_9HYME	98.9	158.52	28	8	1	25,968	Ferritin OS = *Trachymyrmex zeteki* GN = ALC60_04517 PE = 3 SV = 1
A0A0J7KV83_LASNI	98.8	119.94	23	7	2	24,601	Ferritin OS = *Lasius niger* GN = RF55_5701 PE = 3 SV = 1
E2AZU0_CAMFO	96.2	80.69	15	3	3	18,973	Ferritin subunit OS = *Camponotus floridanus* GN = EAG_15045 PE = 4 SV = 1

[a]Percentage confidence score is used to reflect the probability that this protein is correct

[b]The PEAKS protein score (− 10lgP) is calculated as the weighted sum of the − 10lgP scores of the protein's supporting peptides

[c]Percent coverage refers to the percentage value of amino acid residues in the sequence

This alignment allowed the recognition of five of the seven residues involved in ferroxidase activity of the F1HCH chain in the 28 and 31 kDa bands' peptides (Fig. 4a) that are not present in the 26 kDa peptides. Four of them (Y67, E94, E95 and E150) are present in the 31 kDa band and two (E60 and E150) in the 28 kDa band peptides (Fig. 4a and Tables S1 cysteine residue was observed in one of the 31 kDa band peptides from secreted ferritin of adult *C. sericeiventris* ant (Fig. 4a and Table S1 in Online Resource ESM1.pdf). The peptides of the 26 kDa band which were assigned to unique peptides of F2LCH subunit of *Camponotus floridanus* genome sequence are underlined in Fig. 4b.

Ferromagnetic resonance

Figure 5 shows the FMR spectra of ant haemolymph at room temperature (RT), ant haemolymph after the 1st KBr density ultracentrifugation stage (at RT and 100 K) and horse spleen ferritin at 111 K (Wajnberg et al. 2001). The spectra (Fig. 5a–c) of the haemolymph and ferritin obtained from *C. sericeiventris* ants present an incomplete broad line in the low field region (indicated by LF and the dashed curve). The peak of maximum intensity in these spectra is barely noted and the field cross position is in the $g = 6$–11 region. The intense line in the LF region and the broad HF component shown in Fig. 5a, b can be attributed to iron ferritin of ant, as they are observed at RT in the spectra of whole haemolymph and after the 1st density ultracentrifugation stage of purification. This is the only magnetic protein with a magnetic iron core detected by Orbi/Trap MS.

A broad component is also observed in the high field region in the $g = 2$ region (indicated by HF and the dotted curve). This component is a clear asymmetric line with a linewidth of approximately 1100 Oe in the $g = 2.30$ region of the haemolymph spectrum (Fig. 5a) whereas in the ferritin spectrum, the component is narrower (approximately

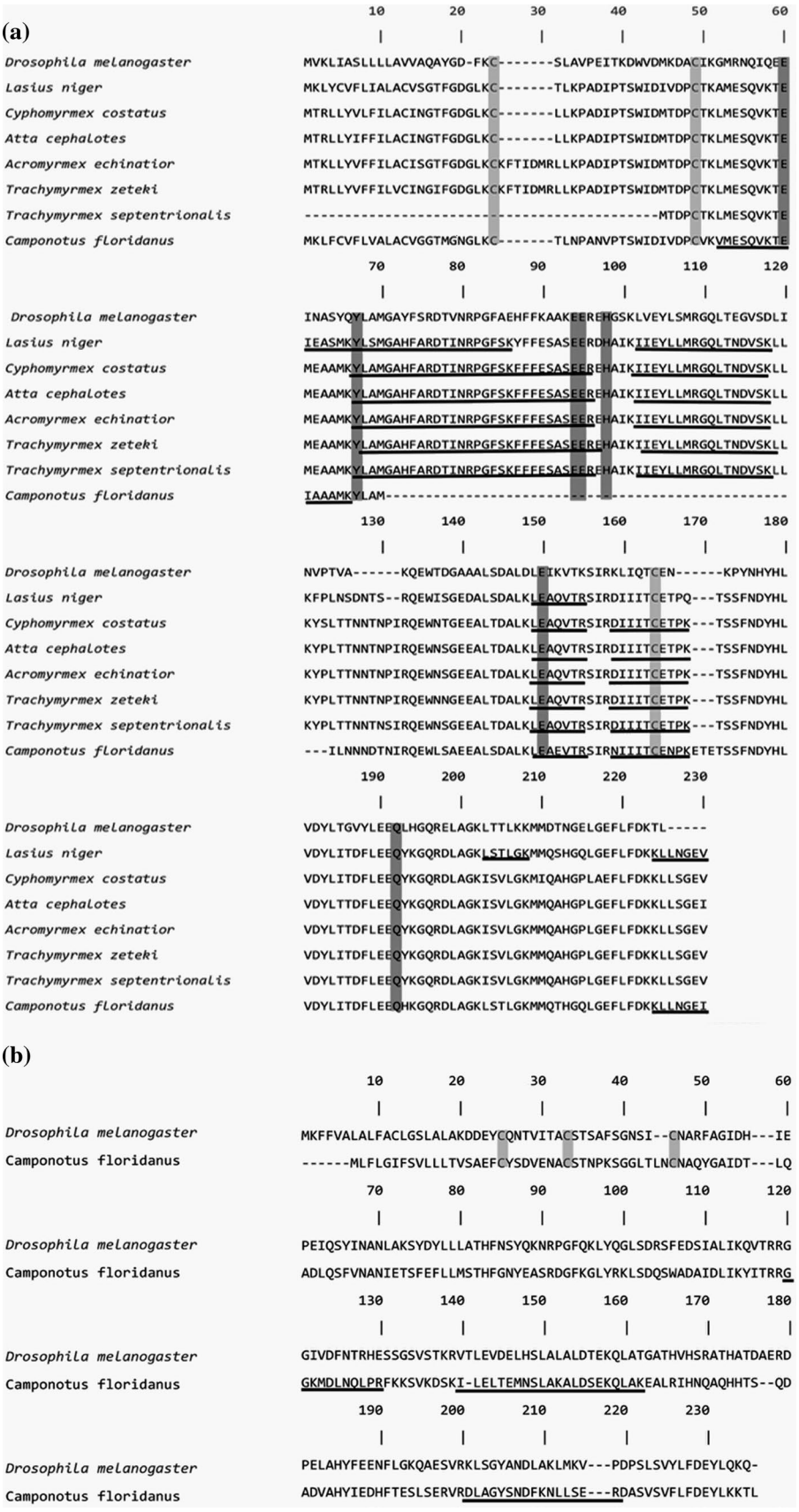

Fig. 4 Sequence alignment by Multialin of ferritin F1HCH subunit from *Formicidae* species which UniProt Accession number sequences are presented in Table 1 and from *Drosophila melanogaster*. Cysteine residues involved in disulfide bonds are shown in light gray. Peptides obtained by Orbi/Trap MS of the 26, 28 and 31 kDa bands identified by Peaks Studio are underlined. **a** F1HCH chain. Residues at the ferroxidase center are highlighted in dark gray; **b** F2LCH chain

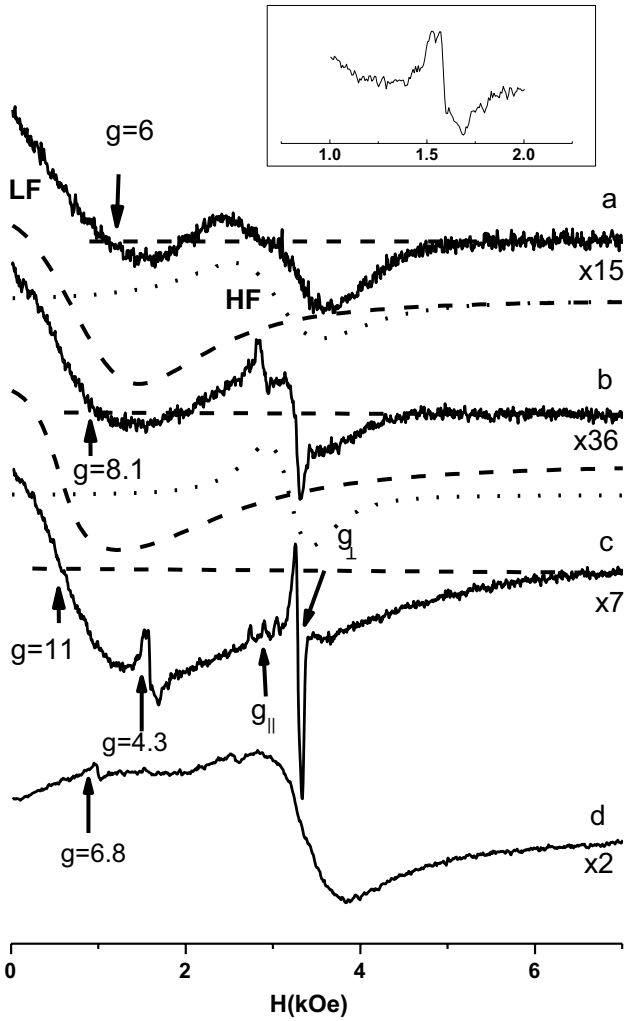

Fig. 5 Ferromagnetic resonance spectra as the derivative of the absorption intensity as a function of the applied magnetic field. a—spectrum of *C. sericeiventris* ant haemolymph at room temperature; b—spectrum of *C. sericeiventris* ant haemolymph after the 1st KBr ultracentrifugation stage at RT and c—same as b, but at 100 K; d—spectrum of horse spleen ferritin at 110 K (Wajnberg et al. 2001). The dashed and dotted curves are guide to the eyes of the broad spectral components. The numbers near the spectra are the multiplying factors used to normalize the spectra to the same acquisition parameters. Inset: amplification of the $g=4$ region of the spectrum c

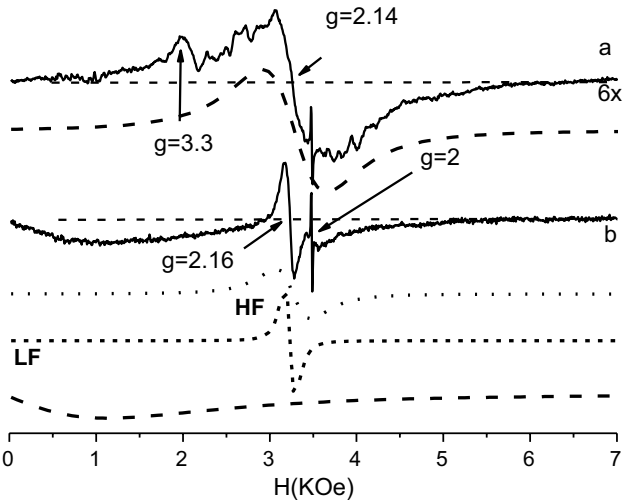

Fig. 6 Ferromagnetic resonance spectra of *C. sericeiventris* ant: a—head; b—thoraxes. The dashed and dotted curves are guide to the eyes of the spectral components fitted to a Lorentzian function. The numbers near the spectra are the multiplying factors used to normalize the spectra to the same acquisition parameters

700 Oe) and is shifted towards the $g=2.11$ region (Fig. 5b). The narrowing of the HF component in the ferritin spectra indicates ferritin iron nanoparticles of different shapes or sizes, or nanoparticles of different constituents from those in the haemolymph, partially eliminated by the purification process.

At 100 K, the ferritin spectrum baseline is not reached until 7 kOe, and the LF component is shifted to lower fields, observed by the zero-crossing magnetic field position at $g=8.4$ to $g=11$ (Fig. 5b, c, respectively). The HF component is absent, and two other narrow paramagnetic signals can be observed at $g=4.3$ and $g=2.0$ (Fig. 5c). The split $g=4.3$ component suggests the presence of an iron-binding protein. An amplification of this and its resonant field line are shown in the inset in Fig. 5. The $g=4.3$ split signal is not typical of isolated iron with rhombic symmetry. It is distinguishable from the nonspecific and featureless signal observed in the $g=6.8$ region in the spectra of horse spleen ferritin at 111 K (Fig. 5d, from Wajnberg et al. 2001), indicating the presence of monomeric iron in natural horse spleen ferritin, which has been suggested to be close enough to the core to be subjected to its magnetic anisotropy field. It indicates the presence of a non-haem protein with a functional mononuclear Fe^{3+} site, such as transferrin that was identified in the electrophoretic band in Fig. 1. This spectral component is in good agreement with the spectrum of transferring extracted from cockroach haemolymph (Gasdaska et al. 1996). The other component is typical of the Cu^{2+} signal with a $g_{\perp}=2.06$ and $g_{//}=2.28$, obtained from the positions indicated by the arrows in Fig. 5c. The field difference between the peaks of the resolved lines indicated that $A_{//}=155$ Oe. It may be associated to Cu^{2+} binding to ferritin as previously suggested in humans (Weir et al. 1985). Copper can also be bound to transferrin as its spectral parameters are very similar to those observed for this complex obtained from cockroach (Gasdaska et al. 1996), although it is not known as a physiologic complex. These two paramagnetic features in the $g=4$ and $g=2$ region do not compromise the ferritin core spectral analysis.

The spectra from the head and thorax (Fig. 6) obtained at RT present a free radical signal at $g=2.0$, a signal typically

observed in biological tissues. Two other lines can be noted in the head spectra: a broad line (linewidth, $\Delta H = 650$ Oe) in the HF region at $g = 2.14$ and a narrow line at $g = 3.3$. Uniquely, the thorax spectrum presents an LF component and the HF component was narrowed to 410 G. Another line ($\Delta H = 115$ Oe) at $g = 2.16$ is also observed only in the thorax spectrum. These broad HF and LF components were associated with isolated nanoparticles and aggregates or large nanoparticles, respectively, in the insect body parts (Wajnberg et al. 2010).

The vertical axes in Figs. 5 and 6 are in arbitrary units. The numbers near the spectra are the multiplying factors used to normalize the spectra in each figure to the same acquisition parameters.

Discussion

While ferritins have been isolated and characterized in a variety of vertebrates, plants and bacteria, relatively little is known about insect ferritin. In this paper, we employed an accepted method used to purify larval stage ferritin (Winzerling et al. 1995) slightly modified to purify it from adult ant haemolymph. To the best of our knowledge, this is the first study to report ferritin extraction from haemolymph of adult ants.

Larval insect ferritin was reported to be relatively stable when subjected to heat, SDS, proteinase K and urea (Nichol et al. 2002; Pham and Winzerling 2010; Winzerling et al. 1995), in contrast to findings reported for ferritin from haemolymph and from the midgut of the butterfly larvae *Calpodes ethlius* (Nichol and Locke 1989). The lack of resistance of ferritin from *C. sericeiventris* to SDS and proteinase K suggests that adult ant ferritin resistance to the physical and chemical agents differs from those of most insect larval phases or it is a minor protein in adult insect haemolymph, such that it was difficult to maintain concentrations that were detectable by electrophoretic methods.

As columns were not adequate for further purification as in previous larval ferritin purification studies (Kim et al. 2001b, 2004), a second KBr density gradient ultracentrifugation step was used. We obtained a yield of approximately 1% of the total haemolymph protein (1.6–3.9 mg/mL) and a ferritin concentration ranging from 0.022 to 0.040 mg/mL, similar to that obtained from *Calpodes ethlius* larval haemolymph (Nichol and Locke 1989) but lower than those obtained from *Manduca sexta* haemolymph (Winzerling et al. 1995).

The MW of insect ferritins, and individual subunits, are frequently reported to be larger than those of vertebrate ferritins. The ferritin isolated from larval haemolymph of *M. sexta*, *C. ethlius*, *G. mellonella* and *Gryllus bimaculatus* was reported to consist of two major subunits with MW from 24 to 32 kDa and different numbers of minor subunits (1–3). 660, 600 and 630 kDa were obtained for the ferritin MW of these insects, except for the field cricket (Winzerling et al. 1995; Nichol and Locke 1989; Kim et al. 2001b; Seo et al. 2004). The MWs of 26, 28 and 31 kDa obtained for the forming subunits of *C. sericeiventris* are consistent with the expected range of insect ferritin.

Our results using non-denaturing electrophoresis (native-PAGE) on a 4–20% gradient gel indicated that the haemolymph ferritin from the adult *C. sericeiventris* ant has a MW greater than 669 kDa, the standard thyroglobulin MW. The absolute MW value cannot be obtained from this result, but if we consider that this ferritin is formed by the same number of 26 and 28 kDa bands (11 of each) and 20% of the 31 kDa minor band (2 subunits), a ferritin MW value of 656 kDa is estimated. This value is in agreement with the 669 kDa lower limit, which suggests that the haemolymph ferritin from adult ants is heavier than vertebrate ferritin and slightly heavier than those of insect larvae.

F1HCH chains of Formicidae ferritin sequences shares a high level of homology as shown for the species in Fig. 4a. This high homology allowed us to identify and to localize the Peaks identification of the *C. sericeiventris* peptides in the ferritin subunits sequences. Both F1HCH and F2LCH chains of the *Trichoplusia ni* moth contain three cysteine each, that is common to other secreted ferritins, but not to cytoplasmic ones (Hamburger et al. 2005). The peptide alignment through Multialin software showed that the F1HCH and F2LCH chains of some Formicidae reported sequences of ferritin also contain these conserved cysteine residues. One of them was observed in one of the 31 kDa band peptides from secreted ferritin of adult *C. sericeiventris* ant (Fig. 4a and Table S1 in Online Resource ESM1.pdf).

As expected, the Formicidae F2LCH chain (Fig. 4b) lacks the residues that define the ferroxidase center, which is present in the F1HCH chain (Fig. 4a). Five of these seven amino acid residues were identified in the 31 kDa band and 28 kDa band peptides. The 26 kDa band peptides were identified as unique in the F2LCH sequence and 31 kDa peptides shares a good level of sequence identity with reported F1HCH subunits of Formicidae sequences. These results strongly support that 31 kDa band is F1HCH and the 26 kDa band is F2LCH. F1HCH and F2LCH peptides were identified in the 28 kDa band peptides, which does not permit to recognize the ferritin subunit.

FMR is a useful technique used to study the magnetic core of ferritin. It has mostly been applied to mammalian ferritins and other iron storage proteins (Wajnberg et al. 2001 and references therein). The LF and HF components are present in the mammalian ferritin spectra and are named features A and B. These features are associated with large and small core particles based on the LF (A) intensity increase relative to the HF component (B) with increasing iron content

and ferritin fractioning in different Fe/protein ratios. The LF component was associated with larger core volumes below their blocking temperature, and consistently shifted to lower fields as the temperature decreased or as the iron/protein molar ratios increased. The HF component was associated with smaller core particles above their blocking temperature. Its field position did not change with temperature (Weir et al. 1985). It is interesting to note that the LF component of the FMR spectrum of ferritin from *C. sericeiventris* ant was similar to that of the magnetite spectra (Ikeya 1993). This finding suggests that magnetite may be present in the insect ferritin core, as observed in the horse ferritin (Gálvez et al. 2008; Cowley et al. 2000).

Differences between ant haemolymph and horse spleen ferritin RT spectra appear in both LF and HF components. These components in the ant spectrum were shifted to lower field positions (higher g values) relative to the horse spleen spectrum that had an LF peak at $g = 4.7$ and an HF component that appeared as an asymmetric line at $g = 2$ (Wajnberg et al. 2001). As expected, at 100 K, the ant ferritin spectrum exhibited a LF component that was shifted to lower field values. Surprisingly, the HF component was no longer visible, probably due to the shifting of this component to low field values, which is consistent with the superparamagnetic behaviour of nanoparticles below their blocking temperature (Ibrahim et al. 1994).

FMR revealed a blocking temperature for horse spleen ferritin of 116 K (Wajnberg et al. 2001). The high iron loading of the ant core is likely associated with a blocking temperature that exceeds 116 K. The observed high relative intensity (LF/HF) of the two spectral components and the disappearance of the superparamagnetic component (HF) at 100 K in the ant ferritin spectra are consistent with this loading hypothesis. Although the two centrifugation steps of the purification method favours iron-rich ferritins, the high LF/HF intensity ratio is also observed in the protein spectra in haemolymph (Fig. 5a), indicating high iron load cores in native ferritin of the ant. In contrast, Gutiérrez et al. (2013) observed that the blocking temperature of pure ferritin from whole *Drosophila* flies obtained by AC magnetic susceptibility is 6.4 K, lower than 20 K of horse ferritin, from magnetization measurements.

The high intensity of the LF component relative to the HF one suggests that the core of adult ant secreted ferritin is mostly iron loaded, in contrast with varied core sizes from non detectable to 48 Å in diameter from ferritin of whole *D. melanogaster* (Gutiérrez et al. 2013).

The comparison of the spectra of ant ferritin to the spectra of human ferritin, which have an iron/protein molar ratio as large as 3000 (Weir et al. 1985), suggests the presence of cores with an iron/ferritin molar ratio greater than 3000 in ant. The iron distribution in insects was only determined for *M. domestica* ferritin. Apoferritin was proposed to be present together with fully loaded protein, with an average iron/ferritin content of 3000 (Capurro et al. 1996). The estimated value for *C. sericeiventris* is consistent with the values reported in *M. domestica* but higher than the values described for *M. sexta* (22 µg of iron/110 µg of protein) (Huebers et al. 1988), which corresponds to an iron/ferritin content of 1750.

The high iron content of the ant ferritin cores in haemolymph could be a characteristic of the secreted ferritins. However, the average iron found in the ferritin core of mice serum (688.9 atoms/molecule) (Cohen et al. 2010) is much lower than our findings in the *C. sericeiventris* core and previous findings in *M. domestica* haemolymph (Capurro et al. 1996), that indicate highly loaded cores of insect secreted ferritin (3000 iron atoms per molecule). Although the ultracentrifugation method effect of eluting ferritin with high iron loaded cores can enhance this difference, it is not determinant as it is a characteristic of the protein in the ant haemolymph. The differences in the blocking temperature and iron loading of the ant and mammal ferritin cores can be due to the intrinsic protein differences. Mammal ferritin is mainly used for the storage and slow release of iron, while the insect protein is used to transfer iron from enterocytes into the haemolymph (Pham and Winzerling 2010). On the other hand, the ferritin origin, that is, from ant haemolymph and from whole *D. melanogaster* fly, that include tissues' ferritin, can account for the apparent discrepancy between ant and fly ferritin blocking temperatures and iron loading relative to horse ferritin.

The signal-to-noise ratio and the signal intensity of the haemolymph and ferritin extracted from approximately 100 ants were too low to be resolved in the spectra of the five ant body parts. As haemolymph is spread throughout the body, the spectral contribution of ferritin in the head and thorax spectra should be similar. Nevertheless, there was no LF contribution in the ant head spectrum, as expected; on the contrary, the LF component was observed in the thorax spectrum. The shape and resonance field of this component differed from those observed in ant ferritin. The baseline, which was not reached in the ant ferritin spectrum, was clear at approximately 6 kOe in the thorax spectrum, and the resonant field was lower than that of ferritin. This result strongly supports the hypothesis that the HF and LF components observed in the spectra of different social insects are associated with isolated magnetic nanoparticles and large or aggregated nanoparticles, which may function as possible magnetic sensors for magnetoreception (Wajnberg et al. 2010) and not a ferritin spectral contribution.

Magnetoreception is an animal sensitivity to the geomagnetic field, perhaps most notably in migratory species that use the Earth's magnetic field to aid in navigation. As in other ant species, magnetoreception may function as one of the orientation mechanisms used by *C. sericeiventris*

ants to guide them back to their tree nest after foraging. Magnetoreception in social insects is still poorly understood. The ferromagnetic hypothesis is well accepted. The presence of magnetic nanoparticles has been shown in different body parts and in the antennae of ants and bees (de Oliveira et al. 2010; Lucano et al. 2006) where they are thought to function as magnetosensors. FMR is mostly used to verify the presence of these magnetic nanoparticles. The ferritin core is antiferromagnetic in mammals. The contribution of insect core ferritin to the FMR spectrum is an open question. The magnetic behaviour of native ferritin depends on the protein source and varies based on differences in the structure and composition of the core. The magnetic properties of the ferritin core in mammals have been subject to extensive investigation over the years; however, aspects of their interpretation remain controversial. The current study successfully isolated, quantified and characterized the ferritin present in adult ant haemolymph. These findings provide significant contributions to future magnetic studies. To the best of our knowledge, the procedure described in this study produced the first FMR spectrum of insect haemolymph ferritin.

The enriched ferritin sample (after 1st KBr ultracentrifugation) obtained in the present study was appropriate for magnetic research purposes, and the yield was comparable to those reported by other studies on insects. Ferritin was identified and validated by proteomic techniques. The FMR results suggested that the iron loading of the ant ferritin core was higher than those reported in the tissue and serum of mammalian ferritins. These results support the necessity of further insect ferritin studies instead of generalizing properties of vertebrate ferritin as an animal model. The structure and properties of insect ferritin associated mainly with iron transport could be adapted for moulting and metamorphosis and could explain the differences in the SDS, proteinase K and urea resistance of larval and adult phase ferritin in insects. The iron transport function of ferritin in insects could account for the high iron content of the core as compared to serum ferritin from mammals, which is believed to be iron poor, and whose main functions are iron overload protection and iron delivery (Sibille et al. 1988). These results should stimulate further studies to characterize the magnetic properties and iron core size distribution of adult ant ferritin, as well as its quaternary structure and the role of the minor subunits.

Acknowledgements We are grateful to Dr. Jacques H. C. Delabie, do Lab. de Mirmecologia do CEPEC, for his assistance with the taxonomic classification of *Camponotus sericeiventris*. M. L. Barriviera was financially supported by Conselho Nacional de Desenvolvimento Científico e Tecnológico. We thank the anonymous reviewers for their constructive comments, which helped us to improve the manuscript and Dr. E. Ellis for linguistic revision.

References

Alenkina IV, Oshtrakh MI, Klencsár Z, Kuzmann E, Chukin AV, Semionkin VA (2014) {^{57}Fe} Mössbauer spectroscopy and electron paramagnetic resonance studies of human liver ferritin, Ferrum Lek and Maltofer®. Spectrochim Acta A Mol Biomol Spectrosc 130C:24–36. https://doi.org/10.1016/j.saa.2014.03.049

Arosio P, Ingrassia R, Cavadini P (2009) Ferritins: a family of molecules for iron storage, antioxidation and more. Biochim Biophys Acta Gen Subj 1790(7):589–599. https://doi.org/10.1016/j.bbagen.2008.09.004

Arosio P, Carmona F, Gozzelino R, Maccarinelli F, Poli M (2015) The importance of eukaryotic ferritins in iron handling and cytoprotection. Biochem J 472(1):1–15. https://doi.org/10.1042/BJ20150787

Atkinson BG, Dean RL, Tomlinson J, Blaker TW (1989) Rapid purification of ferritin from lysates of red blood cells using proteinase-K. Biochem Cell Biol 67(1):52–57. http://www.ncbi.nlm.nih.gov/pubmed/2713128

Bradley JM, Le Brun NE, Moore GR (2016) Ferritins: furnishing proteins with iron Topical Issue in Honor of R.J.P. Williams. J Biol Inorg Chem 21(1):13–28. https://doi.org/10.1007/s00775-016-1336-0

Capurro MDL, Iughetti P, Ribolla PE, de Bianchi AG (1996) Musca domestica hemolymph ferritin. Arch Insect Biochem Physiol 32(2):197–207

Charlesworth A, Georgieva T, Gospodov I et al (1997) Isolation and properties of *Drosophila melanogaster* ferritin—molecular cloning of a cDNA that encodes one subunit, and localization of the gene on the third chromosome. Eur J Biochem 247(2):470–475. http://www.ncbi.nlm.nih.gov/pubmed/9266686

Chasteen ND, Harrison PM (1999) Mineralization in ferritin: an efficient means of iron storage. J Struct Biol 126(3):182–194. https://doi.org/10.1006/jsbi.1999.4118

Chung MCM (1985) A specific iron stain for iron-binding proteins in polyacrylamide gels: application to transferrin and lactoferrin. Anal Biochem 148(2):498–502. https://doi.org/10.1016/0003-2697(85)90258-1

Cohen LA, Gutierrez L, Weiss A et al (2010) Serum ferritin is derived primarily from macrophages through a nonclassical secretory pathway. Blood 116(9):1574–1584. https://doi.org/10.1182/blood-2009-11-253815

Corpet F (1988) Multiple sequence alignment with hierarchical clustering. Nucl Acids Res 16(22):10881–10890

Cowley JM, Dawn EJ, Janney DE, Gerkin RC, Buseck PR (2000) The structure of ferritin cores determined by electron nanodiffraction. J Struct Chem 131:210–216. https://doi.org/10.1006/jsbi.2000.4292

de Oliveira JF, Wajnberg E, Esquivel DMDS, Weinkauf S, Winklhofer M, Hanzlik M (2010) Ant antennae: are they sites for magnetoreception? J R Soc Interface 7(42):143–152. https://doi.org/10.1098/rsif.2009.0102

Dunkov BC, Georgieva T (2006) Insect iron binding proteins: insights from the genomes. Insect Biochem Mol Biol 36(4 SPEC. ISS.):300–309. https://doi.org/10.1016/j.ibmb.2006.01.007

Gasdaska JR, Law JH, Bender CJ, Aisen P (1996) Cockroach transferrin closely resembles vertebrate transferrins in its metal ion-binding properties: a spectroscopic study. J Inorg Biochem 64(4):247–258. https://doi.org/10.1016/S0162-0134(96)00052-9

Gálvez N, Fernández B, Sánchez P, Cuesta R, Ceolín M, Clemente-León M, Trasobares S, López-Haro M, Calvino JJ, Stéphan O, Domínguez-Vera JM (2008) Comparative structural and chemical studies of ferritin cores with gradual removal of their iron contents. J Ann Chem Soc 130(25):8062–8068

Gould JL, Kirschvink JL, Deffeyes KS (1978) Bees have magnetic remanence. Science 201(12):1026–1028. https://doi.org/10.1126/science.201.4360.1026

Gutiérrez L, Zubow K, Nield J, Gambis A, Mollereau B, Lazaro FJ, Mirssilis F (2013) Biophysical and genetic analysis of iron partitioning and ferritin function in *Drosophila melanogaster*. Metallomics 5:997–1005

Hajdusek O, Sojka D, Kopacek P et al (2009) Knockdown of proteins involved in iron metabolism limits tick reproduction and development. Proc Natl Acad Sci 106(4):1033–1038. https://doi.org/10.1073/pnas.0807961106

Hamburger AE, West AP Jr, Hamburger ZA, Hamburger P, Bjorkman PJ (2005) Crystal structure of a secreted insect ferritin reveals a symmetrical arrangement of heavy and light chains. J Mol Biol 349:558–569. https://doi.org/10.1016/j.jmb.2005.03.074

Hsu CY, Chan YP (2011) Identification and localization of proteins associated with biomineralization in the iron deposition vesicles of honeybees (*Apis mellifera*). PLoS One 6(4). https://doi.org/10.1371/journal.pone.0019088

Hsu CY, Li CW (1994) Magnetoreception in honeybees. Science 265:95–97. https://doi.org/10.1126/science.265.5168.95

Hsu C-Y, Ko F-Y, Li C-W, Fann K, Lue J-T (2007) Magnetoreception system in honeybees (*Apis mellifera*). PLoS ONE 2(4):e395. https://doi.org/10.1371/journal.pone.0000395

Huebers HA, Huebers E, Finch CA et al (1988) Iron binding proteins and their roles in the tobacco hornworm, *Manduca sexta* (L.). J Comp Physiol B 158(3):291–300. http://www.ncbi.nlm.nih.gov/pubmed/3192782

Ibrahim MM, Edwards G, Seehra MS, Ganguly B, Huffman GP (1994) Magnetism and spin dynamics of nanoscale FeOOH particles. J Appl Phys 75(10):5873–5875. https://doi.org/10.1063/1.355545

Ikeya M (1993) New application of ESR, dating, dosimetry and microscopy. In: Zimmerman MR, Whitehead N (eds) Silica and silicates. Geotherm and vulcanism, Cap. 10. World Scientific Ed., Singapore

Jung JH, Eom TW, Lee YP, Rhee JY, Choi EH (2011) Magnetic model for a horse-spleen ferritin with a three-phase core structure. J Magn Magn Mater 323(23):3077–3080. https://doi.org/10.1016/j.jmmm.2011.06.060

Kim BS, Lee CS, Yun CY, Yeo SM, Park WM, Kim HR (2001a) Characterization and immunological analysis of ferritin from the hemolymph of *Galleria mellonella*. Comp Biochem Physiol A Mol Integr Physiol. 129(2–3):501–509. https://doi.org/10.1016/S1095-6433(01)00287-2

Kim BS, Yun CY, Yeo SM, Lee HJ, Kim HR (2001b) Cloning and expression of a ferritin subunit for *Galleria mellonella*. Arch Insect Biochem Physiol 47(1):8–17. https://doi.org/10.1002/arch.1030

Kim EY, Lee CS, Kim HR (2004) Purification and properties of ferritin from the last instar larval hemolymph of *Protaetia brevitarsis* (Coleoptera). Entomol Res 34(2):91–99

Kuterbach DA, Walcott B. (1986) Iron-containing cells in the honeybee (*Apis mellifera*). I. Adult morphology and physiology. J Exp Biol 126(1):375–387. http://www.ncbi.nlm.nih.gov/pubmed/3805998

Laemmli UK (1970) Cleavage of structural proteins during the assembly of the head of bacteriophage T4. Nature 227(5259):680–685. https://doi.org/10.1038/227680a0

Lucano MJ, Cernicchiaro G, Wajnberg E, Esquivel DMS (2006) Stingless bee antennae: a magnetic sensory organ? Biometals 19(3):295–300. https://doi.org/10.1007/s10534-005-0520-4

Mandilaras K, Pathmanathan T, Missirlis F (2013) Iron absorption in *Drosophila melanogaster*. Nutrients 5(5):1622–1647. https://doi.org/10.3390/nu5051622

Nichol H, Locke M (1989) The characterization of ferritin in an insect. Insect Biochem 19(6):587–602. https://doi.org/10.1016/0020-1790(89)90024-3

Nichol H, Law J, Winzerling J (2002) Iron metabolism in insects. Annu Rev Entomol 47(1):535–559. https://doi.org/10.1146/annurev.ento.47.091201.145237

Ong ST, Shan Ho JZ, Ho B, Ding JL (2006) Iron-withholding strategy in innate immunity. Immunobiology 211(4):295–314. https://doi.org/10.1016/j.imbio.2006.02.004

Pham DQD, Winzerling JJ (2010) Insect ferritins: typical or atypical? Biochim Biophys Acta Gen Subj 1800(8):824–833. https://doi.org/10.1016/j.bbagen.2010.03.004

Pierre TGS, Tran KC, Webb J et al (1991) Organ-specific crystalline structures of ferritin cores in P-thalassemia/hemoglobin E. 4. Biol Met 4:162–165. https://doi.org/10.1007/BF01141308

Searle BC (2010) Scaffold: a bioinformatic tool for validating MS/MS-based proteomic studies. Proteomic 10(6):1265–1269. https://doi.org/10.1002/pmic200900437

Seo D-H, Nam K-P, Han J et al (2004) Rapid and efficient purification of haemolymph ferritin from cricket, *Gryllus bimaculatus*. Entomol Res 34(1):59–64. https://doi.org/10.1111/j.1748-5967.2004.tb00092.x

Shevchenko A, Wilm M, Vorm O, Mann M (1996) Mass spectrometric sequencing of proteins from silver-stained polyacrylamide gels mass spectrometric sequencing of proteins from silver-stained polyacrylamide gels. Anal Chem 68(5):850–858. https://doi.org/10.1021/ac950914h

Sibille JC, Kondo H, Aisen P (1988) Interactions between isolated hepatocytes and Kupffer cells in iron metabolism: a possible role for ferritin as an iron carrier protein. Hepatology 8:296–301 **[PubMed: 3356411]**

Tang X, Zhou B (2013) Iron homeostasis in insects: insights from *Drosophila* studies. IUBMB Life 65(10):863–872. https://doi.org/10.1002/iub.1211

UniProt Consortium (2017) UniProt: the universal protein knowledgebase. Nucleic Acids Res 45:D158–D169. https://doi.org/10.1093/nar/gkw1099

Wagstaff M, Worwood M, Jacobs A (1978) Properties of human tissue isoferritins. Biochem J 173(3):969–977. http://www.ncbi.nlm.nih.gov/pubmed/708384

Wajnberg E, El-Jaick LJ, Linhares MP, Esquivel DM (2001) Ferromagnetic resonance of horse spleen ferritin: core blocking and surface ordering temperatures. J Magn Reson 153(1):69–74. https://doi.org/10.1006/jmre.2001.2430

Wajnberg E, Acosta-Avalos D, Alves OC, de Oliveira JF, Srygley RB, Esquivel DMS (2010) Magnetoreception in eusocial insects: an update. J R Soc Interface 7(Suppl 2):S207–S225. https://doi.org/10.1098/rsif.2009.0526.focus

Wang W, Knovich M, Coffman L (2010) Serum ferritin: past, present and future. Biochim Biophys Acta 1800(8):760–769. https://doi.org/10.1016/j.bbagen.2010.03.011

Weir MP, Peters TJ, Gibson JF (1985) Electron spin resonance studies of splenic ferritin and haemosiderin. Biochim Biophys Acta (BBA) Protein Struct Mol 828(3):298–305. https://doi.org/10.1016/0167-4838(85)90311-5

Werner WE (1995) Ferguson plot analysis of high molecular weight glutenin subunits by capillary electrophoresis. Cereal Chem 72(3):248–251

Winzerling JJ, Nez P, Porath J, Law JH (1995) Rapid and efficient isolation of transferrin and ferritin from *Manduca sexta*. Insect Biochem Mol Biol 25(2):217–224. https://doi.org/10.1016/0965-1748(94)00058-P